ORGANIC LETTERS

2010
Vol. 12, No. 21
4852−4855

Synthesis and Characterization of Solution-Processable Core-Cyanated Perylene-3,4;9,10-bis(dicarboximide) Derivatives

Shinji Ando, Antonio Facchetti,* and Tobin J. Marks*

Department of Chemistry and the Materials Research Center, Northwestern University, 2145 Sheridan Road, Evanston, Illinois 60208, United States

a-facchetti@northwestern.edu; t-marks@northwestern.edu

Received August 27, 2010

ABSTRACT

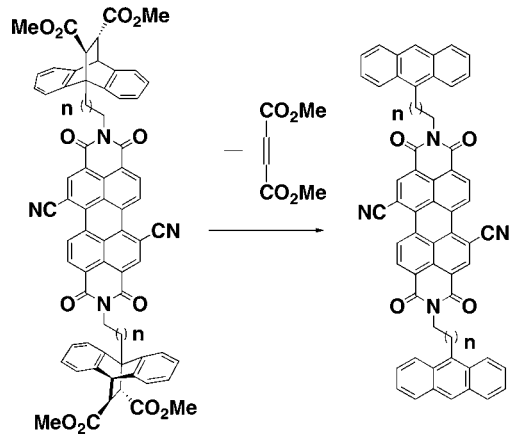

Core-cyanated perylene-3,4;9,10-bis(carboxyimide) derivatives N-functionalized with tethered anthracenes (PDI3A-CN_2, PDI4A-CN_2) and the corresponding solution-processable cycloadduct precursors (PDI3A-CA-CN_2, PDI4A-CA-CN_2) were synthesized and their optical, electrochemical, and thermal properties characterized. These derivatives exhibit HOMO−LUMO energy gaps of ∼2.1−2.3 eV and first reduction potentials between −50 and −150 mV versus SCE. The PDI3A-CN_2 and PDI4A-CN_2 cycloadducts are soluble in common organic solvents (>50 mg/mL), and the corresponding spin-coated films are converted to PDI3A-CN_2 and PDI4A-CN_2 films upon thermal annealing.

Organic semiconductors exhibit unique opto-electronic properties and may find applications in a variety of semiconductor-based devices. One of the most promising characteristics of these materials is the possibility of film and device fabrication using solution-based methodologies that would enable inexpensive, large-area, and flexible electronics. However, as in the case of inorganic semiconductors, the most efficient charge-transporting organic cores are typically those with the closest $\pi-\pi$ stacking and therefore the least soluble in common organic solvents. From these reasons, a variety of molecular design strategies have been explored to enhance solution processability. The most common approach has been core functionalization with organic pendants.[1] Thus, alkyl functionalization of intractable π-conjugated polymers such as polythiophenes and polyphenylenevinylenes affords processable poly(3-hexylthophene) (**P3HT**) and poly[2-(2′-ethylhexyloxy)-5-methoxy-1,4-phenylene vinylene] (**MEH-PPV**) (Figure 1), widely used in field-effect transistors (FETs),[2] light-emitting diodes,[3] and

10.1021/ol1020338
Published on Web 09/30/2010

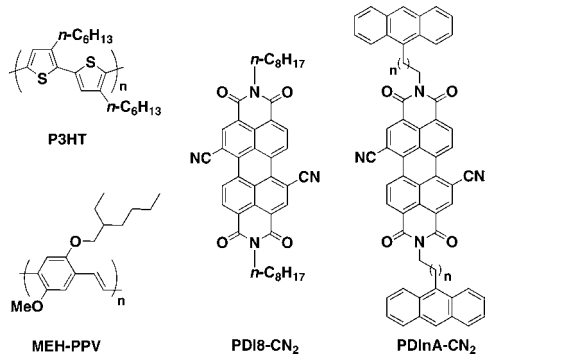

Figure 1. Molecular structures of **P3HT**, **MEH-PPV** and **PDI8-CN_2** and general structure of **PDInA-CN_2**.

photovoltaic cells.[4] An alternative strategy employs a soluble precursor of an insoluble organic semiconductor, depositing the soluble precursor as a thin film and converting it to the insoluble active layer by thermal annealing. In important demonstrations of this approach for organic FET (OFET) fabrication, Müllen and Aftzali et al. synthesized processable cycloadducts of insoluble pentacene. In the first example, films of the tetrachlorocyclohexadiene adduct of pentacene could be converted to pentacene films by heating at 140−220 °C in vacuum, affording FET hole mobilities of 0.01−0.03 $cm^2/(V\ s)$.[5] In a more recent study, mobilities of 0.2 $cm^2/(V\ s)$ were achieved by proper treatment of the substrate-dielectric surface prior to precursor deposition and by optimizing the conversion conditions.[6] In the second example, pentacene precursors were accessed by the Lewis acid-catalyzed Diels−Alder addition of pentacene to heterodienophiles such as *N*-sulfinylalkylmides.[7] These precursors are very soluble in common organic solvents, and conversion to pentacene is achieved by moderate heating. A record hole mobility of 0.89 $cm^2/(V\ s)$ was measured. In another approach, Frechet et al. solubilized oligothiophenes by functionalization with thermally removable branched esters. When solution-cast films of these oligomers are thermolyzed at ∼200 °C, alkene-substituted oligomer films are produced, exhibiting hole field-effect mobilities as high as 0.05 $cm^2/(V\ s)$.[8] Note that these approaches have only been applied to intrinsically *hole-transporting cores* (p-channel materials), and therefore it would be interesting to know whether *electron-transporting* semiconductor (n-channel materials) precursors can also be synthesized.

N,*N*-Dialkyl-2,7-dicyano-3,4:9,10-bis(dicarboxyimide) (**PDIR-CN_2**) derivatives are among the most promising electron-transporting materials for OFET and photovoltaic applications due to their high electron mobilities in ambient and chemical stability. However, despite these advantages,[9] film solution processing is problematic since typical **PDIR-CN_2** solubility is <4 mg/mL (R = *n*-C_8H_{17}, $CH_2C_3F_7$). In this context, we report the design and synthesis of the new cycloadduct-functionalized PDI derivatives **PDI3A-CA-CN_2** and **PDI4A-CA-CN_2** affording, upon retro Diels−Alder reaction, the corresponding alkylanthracenyl-substituted derivatives, **PDI3A-CN_2** and **PDI4A-CN_2**.

The present precursors are designed to achieve good solubility in organic solvents, whereas the products are designed to offer an efficient, established electron-transporting core. Furthermore, the presence of the hole-transporting anthracene unit may promote phase segregation of the molecular subunits in the solid state, resulting in the formation of electron (PDI core) and hole (anthracene unit) conduction pathways, thereby enabling ambipolar transport useful in OFETs and photovoltaics.[10] The solubility of precursor/product can also be tuned via the length of the tethering alkyl chain.

The syntheses of precursors **PDI3A-CA-CN_2** and **PDI4A-CA-CN_2** and products **PDI3A-CN_2** and **PDI4A-CN_2** are outlined in Scheme 1. The starting materials, 1,7-dibromoperylene-3,4:9,10-dianhydride (**PDA-Br_2**) and the aminoalkylanthracenes, were prepared according to known procedures.[11,12] **PDI3A-Br_2** and **PDI4A-Br_2** were synthesized by reacting **PDA-Br_2** with the corresponding alkylamino anthracenes in a xylene−propionic acid mixture.[9b] Then,

(1) (a) Gao, X.; Di, C.; Hu, Y.; Yang, X.; Fan, H.; Zhang, F.; Liu, Y.; Li, H.; Zhu, D. *J. Am. Chem. Soc.* **2010**, *132*, 3697. (b) Suzuki, Y.; Miyazaki, E.; Takimiya, K. *J. Am. Chem. Soc.* **2010**, *132*, 10453. (c) Ortiz, R. P.; Herrera, H.; Blanco, R.; Huang, H.; Facchetti, A.; Marks, T. J.; Zheng, Y.; Segura, J. L. *J. Am. Chem. Soc.* **2010**, *132*, 8440. (d) D. Lai, M.-H.; Chueh, C.-C.; Chen, W.-C.; Wu, J.-L.; Chen, F.-C. *J. Polym. Sci., Part A* **2009**, *47*, 973. (e) Yan, H.; Chen, Z.; Zheng, Y.; Newman, C. E.; Quin, J.; Dolz, F.; Kastler, M.; Facchetti, A. *Nature* **2009**, *457*, 679. (f) Usta, H.; Risko, C.; Wang, Z.; Huang, H.; Deliomeroglu, M. K.; Zhukhovitskiy, A.; Facchetti, A.; Marks, T. J. *J. Am. Chem. Soc.* **2009**, *131*, 5586. (g) Hou, J.; Zhang, S.; Chen, T. L.; Yang, Y. *Chem. Commun.* **2008**, 6034.

(2) (a) Chan, C. K.; Richter, L. J.; Dinardo, B.; Jaye, C.; Conrad, B. R.; Ro, H. W.; Germack, D. S.; Fischer, D. A.; DeLongchamp, D. M.; Gundlach, D. J. *Appl. Phys. Lett.* **2010**, *96*, 133304. (b) Yan, H.; Chen, Z.; Zheng, Y.; Newman, C. E.; Quin, J.; Dolz, F.; Kastler, M.; Facchetti, A. *Nature* **2009**, *457*, 679. (c) Xia, Y.; Cho, J.; Paulsen, B.; Frisbie, C. D.; Renn, M. J. *Appl. Phys. Lett.* **2009**, *94*, 013304.

(3) (a) Perepichka, I. F.; Perepichka, D. F.; Meng, H.; Wudl, F. *Adv. Mater.* **2005**, *17*, 2281. (b) A. Kraft, A.; Grimsdale, A. C.; Holmes, A. B. *Angew. Chem., Int. Ed.* **1998**, *37*, 402.

(4) (a) Cheng, Y.-J.; Yang, S.-H.; Hsu, C.-S. *Chem. Rev.* **2009**, *109*, 5868. (b) Heremans, P.; Cheyns, D.; Rand, B. P. *Acc. Chem. Res.* **2009**, *42*, 1740. (c) Dennler, G.; Sharber, M. C.; Brabec, C. *Adv. Mater.* **2009**, *21*, 1323.

(5) (a) Brown, A. R.; Pomp, A.; de Leeuw, D. M.; Klaassen, D. B. M.; Havinga, E. E.; Herwig, P.; Müllen, K. *J. Appl. Phys.* **1996**, *79*, 2136. (b) Brown, A.; Pomp, R.; Hart, A.; de Leeuw. D. M., C. M. *Science* **1995**, *270*, 972.

(6) Herwig, P. T.; Müllen, K. *Adv. Mater.* **1999**, *11*, 480.

(7) (a) Afzali, A.; Kagan, C. R.; Traub, G. P. *Synth. Met.* **2005**, *155*, 490. (b) Afzali, A.; Dimitrakopoulos, C. D.; Breen, T. L. *J. Am. Chem. Soc.* **2002**, *124*, 8812.

(8) (a) DeLongchamp, D. M.; Sambasivan, S.; Fischer, D. A.; Lin, E. K.; Chang, P.; Murphy, A. R.; Frechet, J. M. J.; Subramanian, V. *Adv. Mater.* **2005**, *17*, 2340. (b) Murphy, A. R.; Frechet, J. M. J.; Chang, P.; Lee, J.; Subramanian, V. *J. Am. Chem. Soc.* **2004**, *126*, 1596.

(9) (a) Piliego, C.; Jarzab, D.; Gigli, G.; Chen, Z.; Facchetti, A.; Loi, M. A. *Adv. Mater.* **2009**, *21*, 1573. (b) Jones, B. A.; Facchetti, A.; Wasielewski, M. R.; Marks, T. J. *J. Am. Chem. Soc.* **2007**, *129*, 15259.

(10) (a) Jonkhejim, P.; Stutzmann, N.; Chen, Z.; Leeuw, D. M. d.; Meijer, E. W.; Schenning, A. P. H. J.; Würthner, F. *J. Am. Chem. Soc.* **2006**, *128*, 9535. (b) Würthner, F.; Chen, Z.; Hoeben, F. J. M.; Osswald, P.; You, C.-C.; Jonkhejim, P.; Herrikhuyzen, J. v.; Schenning, A. P. H. J.; Schoot, P. P. A. M. v. d.; Meijer, E. W.; Beckers, E. H. A.; Meskers, S. C. J.; Janssen, R. A. J. *J. Am. Chem. Soc.* **2004**, *126*, 10611.

(11) Würthner, F.; Stepanenko, V.; Chen, Z.; Saha-Moller, C. R.; Kocher, N.; Stalke, D. *J. Org. Chem.* **2004**, *69*, 7933.

(12) (a) Gardner, R. A.; Delcros, J-.G.; Konate, F.; Breitbeil, F.; Martin, B.; Sigman, M.; Huang, M.; Phanstiel, O. *J. Med. Chem.* **2004**, *47*, 6055. (b) Afonso, C. A. M.; Farinha, J. P. S. *J. Chem. Res. (s)* **2002**, *11*, 584.

Scheme 1. Synthesis of **PDI3A-CA-CN$_2$** and **PDI4A-CA-CN$_2$** Precursors and **PDI3A-CN$_2$** and **PDI4A-CN$_2$**

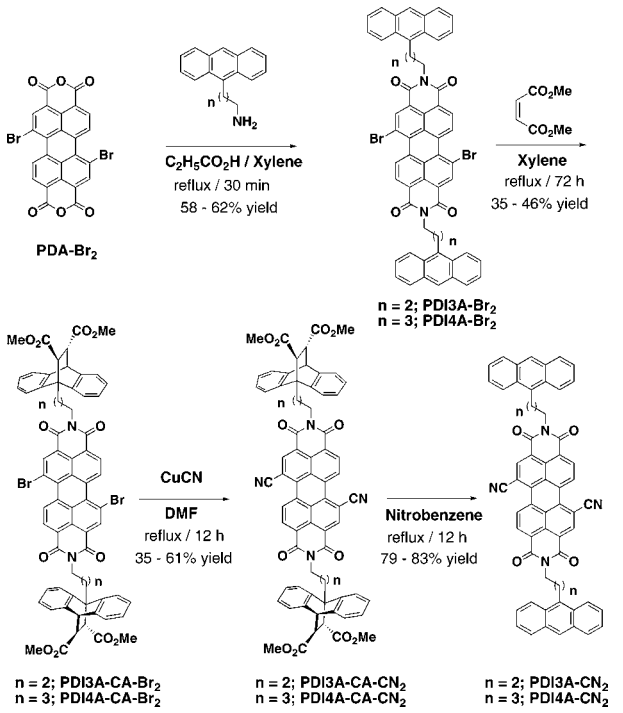

PDI3A-Br$_2$ and **PDI4A-Br$_2$** were reacted with dimethylmaleate in refluxing xylene to afford the soluble Dields−Alder adducts **PDI3A-CA-Br$_2$** and **PDI4A-CA-Br$_2$**. Finally, the cyanated-PDI derivatives **PDI3A-CA-CN$_2$** and **PDI4A-CA-CN$_2$** were obtained by reaction of the corresponding bromo cycloadducts with CuCN in refluxing DMF.[9b] The products were purified by dissolution/reprecipitation from $CHCl_3$/MeOH, isolated as pure purple crystals, and characterized by NMR, MALDI-MS, and elemental analysis. These compounds are very soluble (>50 mg/mL) in chlorinated hydrocarbons, aromatic solvents, and THF. The corresponding insoluble (<1 mg/mL) **PDI3A-CN$_2$** and **PDI4A-CN$_2$** derivatives were synthesized in 79−83% yields via retro Diels−Alder at reflux in nitrobenzene solution. The products were also purified by recrystallization from $C_2H_2Cl_4$. They were characterized by NMR, MALDI-MS, and elemental analysis.

Optical spectroscopic and electrochemical data for new PDI derivatives are summarized in Table 1. Figure 2 shows the optical absorption and emission spectra of the PDI derivatives in solution. All of the compounds exhibit two strong absorptions at 450−550 nm, almost identical to those of the parent **PDI8-CN$_2$**.[9b] The HOMO−LUMO energy gaps obtained from the absorption onsets are almost independent of the core and nitrogen subtitution and are in the 2.1−2.3 eV range very similar to that of **PDI8-CN$_2$**.[9b] In contrast, the emission maxima of **PDInA-Br$_2$** and **-CN$_2$** are shifted to shorter wavelengths versus the Diels−Alder adducts **PDInA-CA-Br$_2$** and **-CN$_2$**, as well as parent **PDI8-CN$_2$**.[9b] Moreover, the anthracene-functionalized derivatives **PDInA-Br$_2$** and **-CN$_2$** exhibit four additional peaks located in the 300−400 nm range due to the absorption of the anthracene π-systems.

Table 1. Optical Absorption and Emission[e] Spectral Data and Electrochemical Redox Potentials[f] for PDI Derivatives

compound	$\lambda_{abs}/\lambda_{em}$ (nm)	E_{gap} (eV)	E^1_{red}/E^2_{red} (V)	E^1_{ox} (V)
PDI3A-CA-Br$_2$	519/542[a]	2.27	−0.38 /−0.68[a]	–
PDI4A-CA-Br$_2$	526/552[b]	2.25	−0.38 /−0.69[a]	–
PDI3A-CA-CN$_2$	522/534[a]	2.11	−0.10 /−0.48[a]	–
PDI4A-CA-CN$_2$	523/543[b]	2.24	−0.12 /−0.50[a]	–
PDI3A-Br$_2$	520/419[a]	2.28	−0.44 /−0.66[c]	+1.39[c]
PDI4A-Br$_2$	526/421[b]	2.23	−0.49 /−0.74[d]	+1.63[d]
PDI3A-CN$_2$	524/421[b]	2.20	−0.06 /−0.47[d]	+1.46[d]
PDI4A-CN$_2$	524/421[b]	2.18	−0.10 /−0.56[d]	+1.48[d]
PDI8-CN$_2$	523/533[b]	2.27	−0.15 /−0.50 [c]	–

[a] In THF. [b] In $CHCl_3$. [c] In CH_2Cl_2. [d] In $C_2H_2Cl_4$. [e] λ_{ex} = 365 nm. [f] E/V vs SCE, 0.1 M n-Bu_4NPF_6, Pt electrode, scan rate 100 mV s^{-1}.

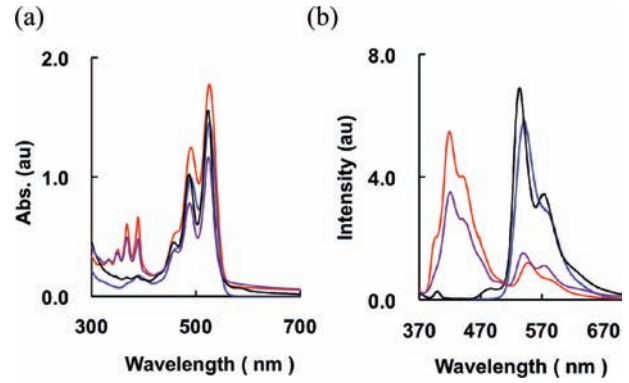

Figure 2. Optical absorption (a) and emission (b) spectra of **PDI3A-CA-Br$_2$** (black), **PDI3A-CA-CN$_2$** (blue), **PDI3A-Br$_2$** (red), and **PDI3A-CN$_2$** (purple) as solutions in THF or $CHCl_3$ solvents.

To monitor the redox properties and electrochemical stability of these systems, cyclic voltammetry experiments were performed, and the results are summarized in Table 1. **PDI3A-CN$_2$** and **PDI4A-CN$_2$** exhibit two reversible reductions at −0.06, −0.47 V and −0.10, −0.56 V, respectively, and a single oxidation at +1.46 and +1.48 V, respectively. The redox potentials of the new core-cyanated derivatives are similar to those of the parent **PDI8-CN$_2$**[9b] and are shifted positive relative to those of the bromo-substituted systems. Similar redox trends are also observed for the Diels−Alder adducts, while anthracene ring-centered oxidation events are not observed.

Figure 3 shows thermogravimetric analysis (TGA) and differential scanning calorimetry (DSC) scans for **PDInA-CA-CN$_2$**. The TGA plots indicate that the retro-Diels−Alder reactions occur at ∼210 °C for **PDI3A-CA-CN$_2$** and at ∼240 °C for **PDI4A-CA-CN$_2$**. The weight loss of ∼24% by ∼290 °C is in agreement with the loss of dimethylmaleate. Moreover, the strong endotherms located at 264 °C for both **PDI3A-CA-CN$_2$** and **PDI4A-CA-CN** are observed in the

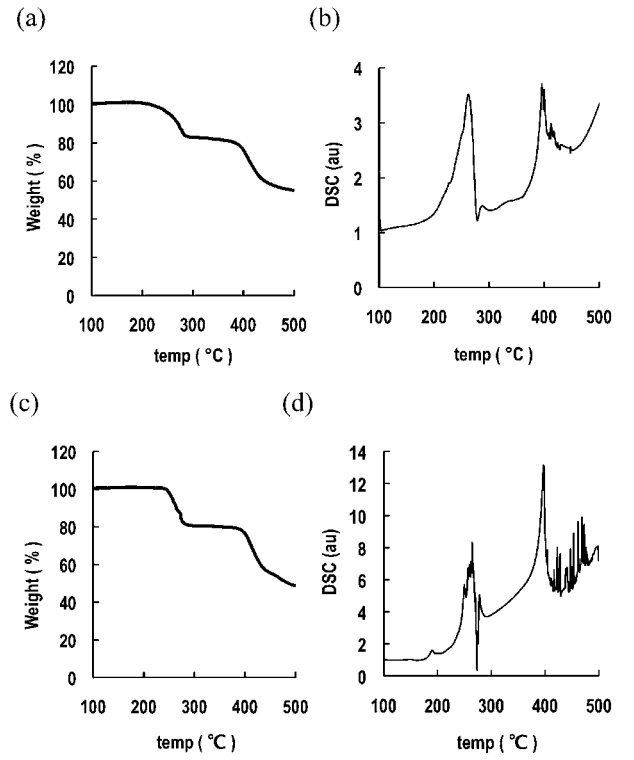

Figure 3. Thermogravimetric analysis data for: (a) **PDI3A-CA-CN_2** and (c) **PDI4A-CA-CN_2** (heating rate: 10 °C/min under N_2). Differential scanning calorimetry data for: (b) **PDI3A-CA-CN_2** and (d) **PDI4A-CA-CN_2** (heating rate: 10 °C/min under N_2).

DSC plots, corroborating the retro-Diels−Alder reaction. The thermal conversion reactions in the solid state were additionaly confirmed by NMR and MALDI after heating solid samples at 300 °C for 30 min.

Additional support for the solid-state thermal conversion of **PDInA-CA-CN_2** portrayed in Scheme 1 was obtained by analyzing the optical spectra before and after annealing. **PDInA-CA-CN_2** films on glass were prepared by spin-coating a 0.8 wt % $CHCl_3$ solution. The films were then heated at 300 °C for 60 min under N_2 to generate the purplish films of **PDInA-CN_2**. Figure 4 shows the film transmission spectra before and after heating. Clearly, the converted films exhibit the characteristic anthracene signature at 300−400 nm.

In summary, we have synthesized new core-cyanated perylene-3,4:9,10-bis(dicarboxyimide) derivatives functionalized with tethered alkyl-anthracenes and their corresponding soluble Diels−Alder cycloadducts. The optical, electrochemical, and thermal properties of these new core-brominated/cyanated derivatives have been characterized. These systems exhibit similar HOMO−LUMO energy gaps and high electron affinities. Diels−Alder reactions on the anthracene rings increase the solubility in organic solvents by >10×, enabling the fabrication of **PDInA-CA-CN_2** films by spin-coating. The films of the precursors can be converted to **PDInA-CN_2** films by heating at 300 °C. Fabrication and detailed characterization of OFETs with this new materials system is currently underway.

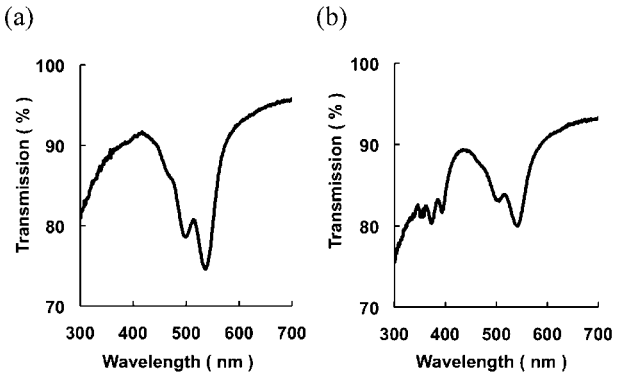

Figure 4. Transmission optical spectra of **PDI3A-CA-CN_2** films (a) before and (b) after thermal annealing.

Acknowledgment. This work was supported by the AFOSR (STTR FA 9550-05-0167) and Polyera Corp. We acknowledge the NSF-MRSEC program (NSF DMR) through the Northwestern Materials Reseach Center for access to characterization facilities.

Supporting Information Available: General experimental methods, ^1H NMR, MALDI-MS, thermal data of **PDInA-CA-CN_2** and **PDInA-CN_2**, and UV−vis, emission spectroscopies, and cyclicvoltammograms for **PDInA-CA-Br_2**, **PDInA-CA-CN_2**, **PDInA-Br_2**, and **PDInA-CN_2**. This material is available free of charge via the Internet at http://pubs.acs.org.

OL1020338